Formation and Bonding of Alane Clusters on Al(111) Surfaces Studied by Infrared Absorption Spectroscopy and Theoretical Modeling

ARTICLE *in* JOURNAL OF THE AMERICAN CHEMICAL SOCIETY · AUGUST 2008

Impact Factor: 12.11 · DOI: 10.1021/ja800136k · Source: PubMed

5 AUTHORS, INCLUDING:

Sylvie Rangan
Rutgers, The State University of New Jersey
67 PUBLICATIONS **663** CITATIONS
SEE PROFILE

James T Muckerman
Brookhaven National Laboratory
237 PUBLICATIONS **6,324** CITATIONS
SEE PROFILE

J|A|C|S
ARTICLES

Formation and Bonding of Alane Clusters on Al(111) Surfaces Studied by Infrared Absorption Spectroscopy and Theoretical Modeling

Santanu Chaudhuri,[†] Sylvie Rangan,[‡] Jean-Francois Veyan,[‡] James T. Muckerman,[§] and Yves J. Chabal*,[‡]

Applied Sciences Laboratory and Institute for Shock Physics, Washington State University, Spokane, Washington 99210-1495, Department of Materials Science and Engineering, University of Texas at Dallas, Richardson, Texas 75080, and Chemistry Department and Center for Functional Nanomaterials, Brookhaven National Laboratory, Upton, New York 11973-5000

Received January 7, 2008; E-mail: chabal@utdallas.edu

Abstract: Alanes are believed to be the mass transport intermediate in many hydrogen storage reactions and thus important for understanding rehydrogenation kinetics for alanates and AlH_3. Combining density functional theory (DFT) and surface infrared (IR) spectroscopy, we provide atomistic details about the formation of alanes on the Al(111) surface, a model environment for the rehydrogenation reactions. At low coverage, DFT predicts a 2-fold bridge site adsorption for atomic hydrogen at 1150 cm^{-1}, which is too weak to be detected by IR but was previously observed in electron energy loss spectroscopy. At higher coverage, steps are the most favorable adsorption sites for atomic H adsorption, and it is likely that the AlH_3 molecules form (initially strongly bound to steps) at saturation. With increasing exposures AlH_3 is extracted from the step edge and becomes highly mobile on the terraces in a weakly bound state, accounting for step etching observed in previous STM studies. The mobility of these weakly bound AlH_3 molecules is the key factor leading to the growth of larger alanes through AlH_3 oligomerization. The subsequent decomposition and desorption of alanes is also investigated and compared to previous temperature programmed desorption studies.

Introduction

Alane clusters (Al_xH_y) are believed to be the ubiquitous intermediates in hydrogen storage reactions for a wide variety of alanates (e.g., $LiAlH_4$, $NaAlH_4$) currently considered for hydrogen storage. The existence and behavior of alanes appear to control and sometimes limit the efficiency of hydrogen storage reactions. Understanding the surface chemistry behind the formation and evolution of alane clusters is therefore important to optimize hydrogen uptake and release for a wide variety of materials for hydrogen storage.

The simplest such material, AlH_3, can store 10 wt.% H_2 and is relatively cheap to manufacture if it can be made reversible under ambient conditions for automobile applications. The community is therefore exploring means to move from the lower gravimetric hydrogen densities currently available in alanates to AlH_3 to meet the Department of Energy's 2010 system target for a hydrogen storage material. The main difficulty for forming AlH_3 or more complex metal hydrides is the dissociation of hydrogen at relatively ambient temperatures. The chemisorption of H_2 on Al has a high activation barrier (>1 eV) for most common surface terminations. Catalytically active Ti centers on Al lower this barrier and act as a pump that generates transient alane species.[1,2] Alanes are, however, highly unstable at the temperatures and pressures at which the regeneration reaction of complex metal hydrides (e.g., $NaAlH_4$) occurs at an optimum rate. For example, alane clusters are highly reactive and, once formed, rapidly react with a "harvesting reagent" such as NaH to form $NaAlH_6$ and $NaAlH_4$ phases.[1] The mechanism of this complex reaction has been the subject of numerous studies, with none pointing definitively to the role that alane clusters play in the decomposition and more importantly in the regeneration process.[3–8]

Alane formation and evolution are difficult to study with spectroscopic and imaging surface science tools. First, in order to avoid formation of aluminum oxide, a clean UHV environment is necessary. Second, instead of a simple monohydride array, a combination of adsorbed H geometries and a wide variety of alanes (AlH, AlH_3, and Al_2H_6, etc.) can be formed simultaneously on aluminum surfaces exposed to atomic

[†] Washington State University.
[‡] University of Texas at Dallas.
[§] Brookhaven National Laboratory.

(1) Chaudhuri, S.; Graetz, J.; Ignatov, A.; Reilly, J. J.; Muckerman, J. T. *J. Am. Chem. Soc.* **2006**, *128* (35), 11404–11415.
(2) Chaudhuri, S.; Muckerman, J. T. *J. Phys. Chem. B* **2005**, *109* (15), 6952–6957.
(3) Bogdanovic, B.; Eberle, U.; Felderhoff, M.; Schuth, F. *Scr. Mater.* **2007**, *56* (10), 813–816.
(4) Bogdanovic, B.; Felderhoff, M.; Kaskel, S.; Pommerin, A.; Schlichte, K.; Schuth, F. *Adv. Mater.* **2003**, *15* (12), 1012.
(5) Bogdanovic, B.; Sandrock, G. *MRS Bull.* **2002**, *27* (9), 712–716.
(6) Graetz, J.; Reilly, J. J.; Johnson, J.; Ignatov, A. Y.; Tyson, T. A. *Appl. Phys. Lett.* **2004**, *85* (3), 500–502.
(7) Gross, K. J.; Thomas, G. J.; Jensen, C. M. *J. Alloys Compd.* **2002**, *330*, 683–690.
(8) Sandrock, G.; Reilly, J.; Graetz, J.; Zhou, W. M.; Johnson, J.; Wegrzyn, J. *Appl. Phys. A: Mater. Sci. Process.* **2005**, *80* (4), 687–690.

10.1021/ja800136k CCC: $40.75
Published on Web 07/18/2008

hydrogen at low temperatures. Paul et al. using electron energy loss spectroscopy (EELS) on an Al(100) surface exposed to atomic hydrogen at 90 K attributes a vibrational feature at 1125 cm^{-1} to hydrogen adsorbed in a 2-fold bridge position.[9] After subsequent anneals to 150 and 280 K, two peaks at higher wavenumber (1750 and 1825 cm^{-1}) emerge and are assigned to the terminal hydrogen stretching modes while a wider peak at 750 cm^{-1} is assigned to a corresponding bending mode.[9] Clear evidence of adsorbed H and the formation of alanes has been seen in temperature-programmed desorption (TPD) studies through H_2 and AlH_n^+ fragment desorption around 340 K from aluminum surfaces exposed to atomic hydrogen but only for temperature ramping rates above 10 K/s.[10] For lower ramping rates, only H_2 is desorbed at 340 K, showing that the adsorbed species are unstable and are undergoing transformations with possible cracking of the alanes into Al metal with concomitant H_2 release.[10,11] A minimum hydrogen exposure appears to be necessary to see alane fragment desorption, while H_2 desorption is always observed, consistent with the existence of adsorbed atomic H at low coverage and the formation of alanes at higher coverage.[11] Once formed, the alanes should be highly mobile species at or near room temperature (with calculated diffusion rates around 5.29×10^{-5} cm/s at 300 K).[1] In order to study the formation of alanes, lower temperatures and high vacuum conditions are needed for spectroscopic probes. This is a very different environment compared to the range of temperatures and hydrogen pressures needed for aluminum hydride formation.

Imaging of alanes on surfaces is equally difficult. The only attempt to observe alanes using a scanning tunnel microscope (STM) has been made at 300 K on a surface previously dosed at low temperature.[12] It was found that alanes lack contrast under electron microscopes. Moreover the STM tips can be modified by the reactive alane clusters during attempts to image the surface reaction under controlled conditions. As a result, the interpretation of such images can be hindered by artifacts arising from unknown modifications to the local densities of states when probed with alane-modified STM tips.[12] Probes are therefore needed that can distinguish various alanes.

Infrared spectroscopy has proven to be sensitive enough to investigate the adsorption of hydrogen and other molecules on metal and semiconductor surfaces, providing detailed information regarding the chemical nature of the resulting surfaces, adsorbate states, and mechanisms of adsorbate-driven chemical reactions at surfaces.[13–22] The alane species are characterized by distinct IR active vibrations in the gas phase[23] and retain some of their IR signatures when adsorbed on Al surfaces. The interpretation of IR spectra is however very difficult. An early study combining IR spectroscopy at 180 K and subsequent STM imaging after annealing at 300 K proposed an assignment of observed IR modes based on a general identification of modes in gas-phase clusters.[12] However this approach neglects the modification of cluster geometries and electronic structures upon adsorption on the aluminum surface. As will be shown in this study, combining IR spectroscopy and first-principles calculations of atomistic models of chemisorbed and physisorbed alanes on an aluminum surface constitutes a powerful approach to understanding alane formation on Al surfaces.

The aim of the present work is to provide atomistic details about the formation of alane clusters that could ultimately lead to synthesis of the bulk AlH_3 phase in the absence of alane harvesting reagents such as NaH. Combining density functional theory (DFT) and surface infrared (IR) spectroscopy to study the formation and temperature dependent evolution of alanes on Al(111) surfaces, two important aspects can be addressed that directly impact the roles of alanes: (a) identification of different possible ways in which alanes can be adsorbed on the Al(111) surface, and (b) the mechanism of oligomerization of alanes (i.e., from smaller to larger clusters) as a function of temperature and hydrogen coverage. Although the use of well oriented (111) surfaces provides a simple template, the active interaction of atomic hydrogen with aluminum quickly complicates the situation, with the formation of steps and defects. As a result, alanes can be formed on (111) terraces or steps or from more complex microfacets. Moreover, the adsorption strength of alanes can vary, adding to the complexity of the system (i.e., IR spectra). Computational modeling has therefore been expanded to explore a wide range of surface environments. Since an exhaustive study of *all* clusters and possible metastable binding arrangements cannot be realistically carried out, the identification of the most common environments and stable binding geometries for a small subset of alanes was performed. The understanding of the formation, binding energy, stability, and temperature dependent mobility of alane clusters developed here will hopefully constitute a basis for finding rational ways of regenerating alanates or bulk AlH_3 under ambient conditions.

Experimental Section

Experimental Techniques. The experiments were performed on $2.5 \times 1.0 \times 0.2$ cm^3 commercially produced Al(111) single crystals with one face mechanically and electrochemically polished. A sample was placed in a UHV chamber with a base pressure of 2×10^{-10} Torr, equipped with *in situ* LEED, AES, and IR reflection absorption spectroscopy (IRRAS). The cleanliness of the sample was achieved by a thorough degassing, followed by several cycles of Ar^+ ion sputtering at 500 eV while maintaining the sample temperature at 100 °C and a short subsequent annealing at 400 °C. Because of the high mobility of Al atoms on the Al(111) surface, the short annealing step at 400 °C allows the surface to reconstruct but avoids recontamination that occurs when annealing is too long. The cleanliness of the sample was checked by AES at 3 KeV: after

(9) Paul, J. *Phys. Rev. B* **1988**, *37* (11), 6164.
(10) Hara, M.; Domen, K.; Onishi, T.; Nozoye, H. *J. Phys. Chem.* **1991**, *95* (1), 6–7.
(11) Winkler, A.; Pozgainer, G.; Rendulic, K. D. *Surf. Sci.* **1991**, *251*, 886–890.
(12) Go, E. P.; Thuermer, K.; Reutt-Robey, J. E. *Surf. Sci.* **1999**, *437* (3), 377–385.
(13) Chabal, Y. J.; Dumas, P.; Guyot Sionnest, P.; Higashi, G. S. *Surf. Sci.* **1991**, *242* (1−3), 524–530.
(14) Chabal, Y. J.; Hines, M. A.; Feijoo, D. *J. Vac. Sci. Technol. A* **1995**, *13* (3), 1719–1727.
(15) Dumas, P.; Chabal, Y. J.; Jakob, P. *Appl. Surf. Sci.* **1993**, *65−6*, 580–586.
(16) Dumas, P.; Weldon, M. K.; Chabal, Y. J.; Williams, G. P. *Surf. Rev. Lett.* **1999**, *6* (2), 225–255.
(17) Eng, J.; Raghavachari, K.; Struck, L. M.; Chabal, Y. J.; Bent, B. E.; Flynn, G. W.; Christman, S. B.; Chaban, E. E.; Williams, G. P.; Radermacher, K.; Manti, S. *J. Chem. Phys.* **1997**, *106* (23), 9889–9898.
(18) Fukidome, H.; Pluchery, O.; Queeney, K. T.; Caudano, Y.; Raghavachari, K.; Weldon, M. K.; Chaban, E. E.; Christman, S. B.; Kobayashi, H.; Chabal, Y. J. *Surf. Sci.* **2002**, *502*, 498–502.
(19) Hines, M. A.; Chabal, Y. J. *Abstr. Pap.—Am. Chem. Soc.* **1993**, *206*, 101.
(20) Jakob, P.; Chabal, Y. J.; Raghavachari, K. *J. Electron. Spectrosc.* **1993**, *64−5*, 59–66.
(21) Morral, A. F.; Zahler, J. M.; Griggs, M. J.; Atwater, H. A.; Chabal, Y. J. *Phys. Rev. B* **2005**, *72* (8), 085219.
(22) Reutt Robey, J. E.; Doren, D. J.; Chabal, Y. J.; Christman, S. B. *J. Chem. Phys.* **1990**, *93* (12), 9113–9129.
(23) Andrews, L.; Wang, X. F. *J. Phys. Chem. A* **2004**, *108* (19), 4202–4210.

several sputtering cycles, oxygen and carbon were not detectable anymore. The first sample was a flat Al(111) surface, characterized by a sharp LEED pattern at energies up to 400 eV; the second sample, repolished after deformations due to overheating, is characterized by a high density of steps displaying similar adsorption behavior than that of a more regularly stepped surfaces.[12]

A mid-infrared modulated beam is generated by a Fourier transform interferometer. After reflection on a focusing mirror, it penetrates the experimental chamber through a KBr window and is focused on the crystal surface with a glancing angle of 5°. After reflection from the sample surface, the beam exits the chamber through another KBr window and is refocused on a DTGS infrared detector. The IRRAS system, from the IR source to the entrance window is maintained under vacuum of around 10 Torr outside the UHV chamber. The exit refocusing mirror and the detector are maintained in a dry N_2 atmosphere. The nominal resolution is 4 cm^{-1} using Happ-Genzel apodization. The temperature of the sample is controlled by a combination of liquid nitrogen cooling and indirect heating using a W filament on the back of the sample, and is measured using a K-type thermocouple directly in contact with the sample. The temperature range can be varied from 90 K to 730 K. During atomic H exposures, the experimental chamber is filled with molecular hydrogen at pressures in the range of 1×10^{-6} Torr. A 1.5 cm tungsten filament placed 8 cm from the Al surface and held at 2000 K dissociates the molecular hydrogen. The dose during exposure in Langmuir (L) is obtained using an uncorrected reading of the H_2 pressure by the ion gauge. In our setup, the surface saturation, measured to be 1.6 monolayer (ML) by previous TPD experiments (a H coverage greater than 1 ML is due to the formation of alanes), is reached at roughly 600L.[11] Assuming a linear dependence between exposure and coverage, we can therefore estimate that 1L exposure leads to 0.3% of a monolayer. The temperature elevation of the sample due to the hot W filament (used to dissociate H_2 during H dosing) is less than 1° for 15 s exposures and less than 10° for 120 s exposures.

Theoretical Methods. The theoretical model of the surface termination is a 11.45 × 11.45 Å Al(111) slab corresponding to a (4 × 4) unit cell. There are in total five atomic layers with the top three allowed to relax upon adsorption of alane clusters. Increasing the number of atomic layers beyond the current level improves the Al(111) surface energy very little but adds to the computational expense of an already relatively large unit cell. To calibrate the accuracy of subsequent calculations of somewhat lower quality, the structures of the alane clusters were first calculated at the B3LYP/6−311+G*(5D, 7F) level of theory using the Gaussian03 program. The gas-phase IR spectrum of each alane species was then computed. The subsequent surface calculations were performed with the DMOL3 program[24,25] to predict structures and IR spectra using the all-electron DND basis set (equivalent to a double ζ basis set) and the RPBE exchange/correlation functional.[26] The gas-phase clusters were reoptimized on the surface to investigate their binding orientations and to calculate partial Hessian matrices from their optimized geometries. Because of the relatively large unit cell size, a Γ-centered 2 × 2 k-mesh was sufficient to provide optimized energies for the clusters adsorbed on a periodic Al(111) slab. The calculated vibrational frequencies were tabulated for different surface environments such as terraces and atomic steps. Both chemisorbed (strongly bound) and physisorbed (loosely bound) clusters were investigated to determine the influence of the binding configuration on the vibrational spectrum. The harmonic vibrational frequencies were calculated from the diagonalized (second derivative) mass-weighted **F** matrix expressed traditionally as follows:

$$\mathbf{F}_{ij} = \frac{1}{\sqrt{m_i m_j}} \frac{\partial^2 E}{\partial q_i \, \partial q_j} \tag{1}$$

where q_i and q_j represent the Cartesian coordinates, and m_i and m_j are the masses of the atoms with which they are associated. The square roots of the eigenvalues of the **F** matrix are the harmonic frequencies. As evident from the nature of these calculations, the calculated forces need to be highly accurate. This is also the reason behind using an all-electron DFT method compared to an ultrasoft pseudopotential-DFT method. One particular problem with partial Hessian calculations is that they do not provide a reliable estimate of intensities, and thus we used experimental IR spectra and the calculated intensities from the gas-phase clusters as a guide. We started Broyden–Fletcher–Goldfarb–Shanno (BFGS) optimizations using the DND basis set[27] from two initial configurations: (a) the clusters placed horizontal to the surface, and (b) the clusters placed in a vertical position with the terminal hydrogen pointing toward the surface Al atoms, all within the Van der Waals radii of the atoms involved. The aim here was to find the ground-state minima closest to these configurations since each cluster can have many different configurations with comparable binding energy.

We have carried out these calculations on the first three members of the alane family of clusters, i.e., AlH_3, Al_2H_6 and Al_3H_9 as gas-phase clusters to compare the accuracy of our models with previously published experimental and calculated data. We find that our calculated frequencies are slightly different from the experimentally observed lines, but the deviations are consistent within our calculations and with other published theoretical results. For example, the four highest-frequency modes (b_{1u} and b_{3u} modes) for a gas-phase Al_2H_6 cluster were observed at 1932, 1915, 1408, and 1268 cm^{-1} by Andrews et al.[23] and are at 1958, 1932, 1416, and 1331 cm^{-1} in our calculations, i.e., calculated at systematically higher frequencies. In the gas-phase optimization, the hybrid B3LYP method often favors symmetric clusters compared to results using a pure DFT method with the DND basis. The DFT/DND method fails to represent the higher frequency combination modes of the symmetric Al_3H_9 cluster as shown in Table 1, and thus we believe the B3LYP values are a better representation of the experimentally observed values for larger alane clusters.

For comparison, we also carried out constrained symmetric optimization calculations of alanes using pure DFT with DND basis sets. The gas-phase optimized clusters were allowed to relax to their minima on an Al(111) surface in two different surface environments: (a) a flat periodic terrace, and (b) an atomic step running parallel to one of the vectors that form the surface unit cell. The terraces are representative of an ideal single-crystal Al surface, and the steps are representative of surface roughness and imperfections that would be generated by the formation of alane clusters. Each cluster was optimized in these two different surface environments. Depending on the cluster size and geometry, the binding orientations and the adsorption energies differ widely. The spectra of calculated vibrational frequencies also become more complex with increasing cluster size. Even the physisorbed clusters are slightly different from their gas-phase analogues. The binding or absorption energies were calculated as a difference between total energies of the alane-chemisorbed surface and the bare flat periodic Al(111) surface or the surface with an atomic step plus the isolated gas-phase cluster energies. For consistency, energies of the corresponding gas-phase clusters are calculated in vacuum inside a unit cell of the same dimension used for the periodic surface calculations. It is also known that alanes can have molecular formulas different from $(AlH_3)_x$. One such class that has recently attracted interest is the so-called *closo*-alanes[28] represented as Al_4H_4 and Al_nH_{n+2} where $4 \leq n \leq 8$. We have therefore calculated the geometry and vibrational modes for the Al_4H_6 cluster[29] from this series and find that it would be quite stable on an Al surface as well.

(24) Delley, B. *J. Chem. Phys.* **1990**, *92*, 508.
(25) Delley, B. *J. Chem. Phys.* **2000**, *113*, 7756.
(26) Hammer, B.; Hansen, L. B.; Norskov, J. K. *Phys. Rev. B* **1999**, *59* (11), 7413–7421.
(27) Pfrommer, B. G.; Cote, M.; Louie, S. G.; Cohen, M. L. *J. Comput. Phys.* **1997**, *131* (1), 233–240.
(28) Grubisic, A.; Li, X.; Stokes, S. T.; Cordes, J.; Gantefor, G. F.; Bowen, K. H.; Kiran, B.; Jena, P.; Burgert, R.; Schnockel, H. *J. Am. Chem. Soc.* **2007**, *129* (18), 5969–5975.

Table 1. The Vibrational Frequencies of Alane Clusters Calculated Using Gas-Phase B3LYP and DFT/DND in a Periodic Box Technique Compared to Experimentally Observed Values[a]

AlH_3			Al_2H_6			Al_3H_9		
DND[b]	B3LYP[c]	obsd[d]	DND[b]	B3LYP[c]	obsd[e]	DND[b]	B3LYP[c]	obsd[f]
696(328)	708(333)	697	616(243)	631(253)	632(0.039)	552 (156)	715(1118)	726
781(200)	800(217)	783	700(588)	717(615)	702(0.048)	556 (151)	794(282)	851
782(199)	800(217)	1882	835(205)	852(193)	836(0.037)	671 (533)	907(763)	1817
1890(26)	1936(0)		1245(347)	1285(308)	1268(0.053)	677 (533)	1905(1266)	1920
1903(267)	1945(271)		1332(0)	1479(1051)	1408(0.0128)	770(299)	1982(542)	1942
1914(257)	1945(271)		1417(1025)	1963(128)	1915(0.023)	859(403)	1988(278)	
			1932(142)	1983(390)	1931(0.069)	864(407)		
			1959(422)			1813 (1334)		
						1815.5 (1332)		
						1903 (44)		
						1904 (24)		
						1915.6 (552)		

[a] The relative intensities of the calculated modes in km/mol units are indicated in parentheses. Only the modes with detectable intensity in the experimental spectra are displayed. [b] Calculated in a periodic box (this work) [c] Calculated as a gas-phase cluster using a 6−311+G*(5D, 7F) basis set (this work) [d] Values from the work by Kurth et al.[38] [e] Values from the work by Wang et al.[23] [f] Values from the theoretical work by Duke et al.[39]

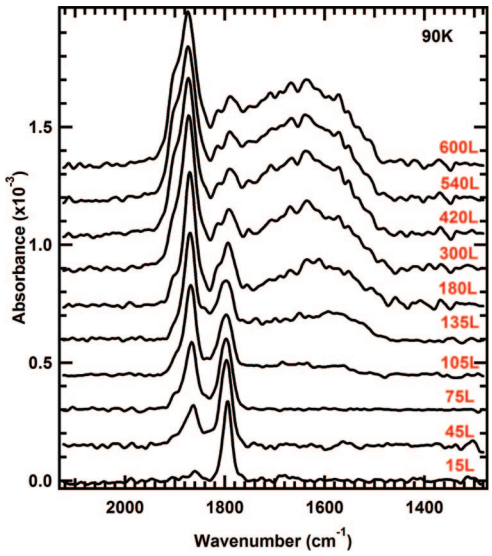

Figure 1. FTIR spectra shown in absorbance as a function of the photon wavenumbers (cm^{-1}) of a highly stepped Al(111) surface, sequentially exposed to atomic hydrogen at 90 K. The dose in Langmuir is obtained using an uncorrected reading of the H_2 pressure by the ion gauge.

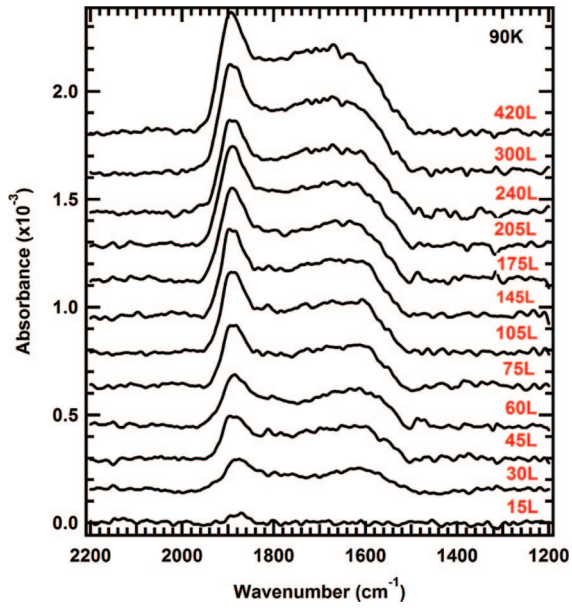

Figure 2. FTIR spectra shown in absorbance as a function of the photon wavenumbers (cm^{-1}) of a flat Al(111) surface, sequentially exposed to atomic hydrogen at 90 K. The dose in Langmuir is obtained using an uncorrected reading of the H_2 pressure by the ion gauge.

Results

Experimental Results. 1. 90 K Experiments. In Figures 1 and 2, the FTIR spectra recorded after exposure at 90 K are shown for both highly stepped, and flat Al(111) surfaces, respectively. The absorbance (*y*-axis) is plotted as a function of the photon wavenumber in cm^{-1} (*x*-axis) showing the effects of sequential exposures to atomic hydrogen.

On the highly stepped surface (Figure 1), a 15 s exposure to atomic hydrogen at 10^{-6} Torr (i.e., 15L of H_2 gas) gives rise to a strong IR band, centered at 1795 cm^{-1} with a full width at half maximum (fwhm) of 22 cm^{-1}, with a small peak also present on the high-frequency side of it (around 1860 cm^{-1}). With increasing coverages, this second peak sharpens and blue shifts to 1874 cm^{-1}, while the 1795 cm^{-1} band broadens, possibly splitting into several components. For coverages above 75L, a shoulder in the higher-wavenumber region around 1900 cm^{-1} and a broad feature centered around 1600 cm^{-1} seem to grow simultaneously with increasing exposures. Beyond 600L, the IR absorption spectrum remains stable. All these IR spectra are stable with time for at least the several hours necessary to acquire all the spectral data.

On the flat Al(111) surface, the situation (Figure 2) is somewhat different. For a 15L exposure, there is no feature at 1795 cm^{-1}, only a small band centered at 1870 cm^{-1}. With increasing coverage, it appears that the spectra are composed of a broadened version of the three main features described previously for the stepped surface, and that these features grow simultaneously. Since the overall spectrum is much broader, it is not possible anymore to distinguish between the peak at 1874 cm^{-1} and the high-wavenumber shoulder.

Several observations can be made at this point. First, the presence of multiple vibrational modes suggests that several adsorbed species most likely coexist on the surface at 90 K. The existence and concentration of these adsorbed species strongly depend on the coverage and on the topography of the Al(111) surface. The different IR features appear sequentially on the highly stepped Al(111) surface, whereas they all appear

(29) Li, X.; Grubisic, A.; Stokes, S. T.; Cordes, J.; Gantefor, G. F.; Bowen, K. H.; Kiran, B.; Willis, M.; Jena, P.; Burgert, R.; Schnockel, H. *Science* **2007**, *315* (5810), 356–358.

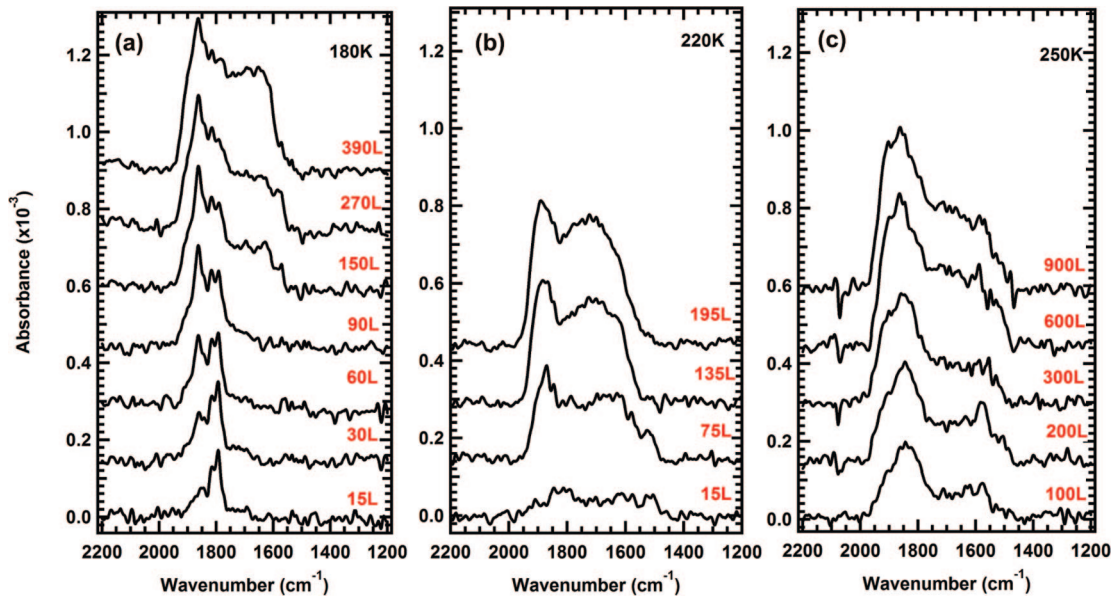

Figure 3. FTIR spectra shown in absorbance as a function of the photon wavenumbers (cm^{-1}) of a stepped Al(111) surface, sequentially exposed to atomic hydrogen at (a) 180 K, (b) 220 K and (c) 250 K. The dose in Langmuir is obtained using an uncorrected reading of the H_2 pressure by the ion gauge.

simultaneously on the flat surface (within our observation time scale). The morphology of the Al(111) surface is therefore a key parameter in the kinetic process of H adsorption. Second, the absorption features are very broad possibly due to the overlap of multiple IR transitions, in particular on the flat surface. This may be due to multiple adsorption modes, multiple adsorption sites due to the disorder induced during the initial adsorption process, interadsorbate interactions, or differences in the chemical bonds of different adsorbed species. In particular, large alanes will always possess terminal and bridge hydrogen atoms, all with correspondingly close but not necessarily identical frequencies.

2. Thermal Stability. IR spectra have been taken during sequential dosing of both Al surfaces at three different substrate temperatures: 180 K, 220 K and 250 K. The results are shown in Figure 3 for the highly stepped Al surface. The relatively high noise level is due to the fact that the filament located behind the sample is hot, to maintain the temperature, generating a strong IR radiation with electrical noise. For the stepped surface, the IR spectra at 180 K (Figure 3a) are similar to spectra taken at 90 K (Figure 1). The peak centered at 1795 cm^{-1} is still dominant for low exposures, the feature at 1874 cm^{-1} appears at higher exposures, followed by a high-wavenumber shoulder and a broad peak around 1600 cm^{-1} above 90L. At 220 K the IR spectrum is weak and broad already at 15L (Figure 3b). At higher exposures, broad lines appear around 1880 cm^{-1} and above 1600 cm^{-1} similar to what is observed when dosing a flat Al surface at 90 K. At 250 K, IR absorption is only observed for high exposures (see Figure 3c). Moreover, there is a progressive loss of this absorption signal, indicating the hydrogen species are unstable with time. The shape of the spectra is also altered, with a larger contribution of high-wavenumber spectral components above 1900 cm^{-1} and a partial loss of the 1600 cm^{-1} broad feature.

The IR spectra obtained on the flat surface at 180 K (not shown) are similar to the one measured at 90 K on the same surface. At 220 K (not shown) and 250 K (not shown) the spectra are essentially similar except for a slightly higher contribution from the broad 1600 cm^{-1} line. This behavior is much different from the one observed on the stepped surface.

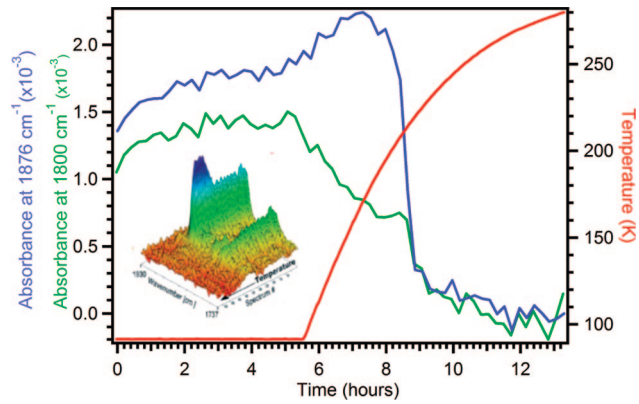

Figure 4. Intensity variation of the 1876 cm^{-1} and 1800 cm^{-1} mode intensities (integrated over the range ± 5 cm^{-1} around 1876 cm-1 and 1800 cm^{-1}) after 150L H dose on a stepped surface as a function of time while the sample warms up from 90 K to 300 K at a rate lower than 0.1 K/s. The inset shows the series of FTIR spectra taken during this process.

3. Thermal Desorption. There is an apparent inconsistency between the temperature-programmed desorption (TPD) results in the literature (showing a desorption peak around 340 K) and our FTIR data, indicating a strong loss of absorption below 250 K. We have therefore monitored the IR absorption spectra after dosing as a function of substrate temperature, being limited to a very slow temperature ramp to avoid damage to our large sample. The series of IR spectra shown in Figure 4 is averaged for 20 min while the Al sample is warming up from 90 K to room temperature. The intensity variation of the most relevant lines can then be followed as a function of the temperature.

Figure 4 shows the intensities of the 1800 cm^{-1} and 1876 cm^{-1} bands (integrated over the range ± 5 cm^{-1} around 1800 cm^{-1} and 1876 cm^{-1}) and the sample temperature variation for the stepped Al surface dosed at 150L (i.e., not fully saturated). The inset shows the corresponding IR spectra displayed in three dimensions to show the time progression (spectrum no.). Interestingly, the 1800 cm^{-1} feature decreases above 110 K while the 1876 cm^{-1} feature increases strongly to reach a maximum at 160 K. This observation suggests a transformation

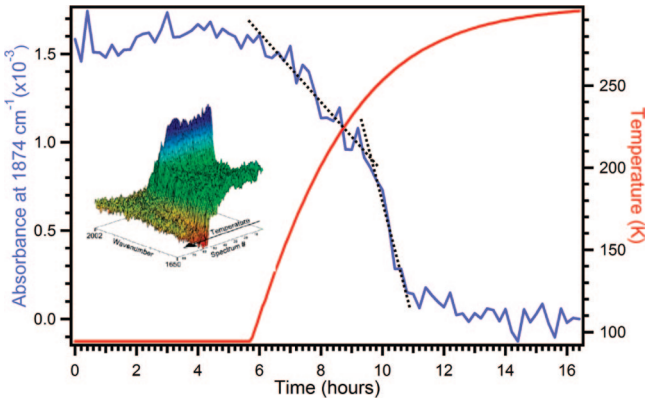

Figure 5. Intensity variation of the 1874 cm^{-1} mode intensity (integrated over the range ± 5 cm^{-1} around 1874 cm^{-1}) after 150L H dose on a stepped surface as a function of time while the sample warms up from 90 K to 300 K at a rate lower than 0.1 K/s. The inset shows the series of FTIR spectra taken during this process.

from one adsorbed species with a characteristic IR signal around 1800 cm^{-1} to another species with an IR signature around 1876 cm^{-1}. The absorbance of both types of species decreases quickly to zero as the temperature increases beyond 220 K. The situation is different for full hydrogen saturation of the same stepped surface as shown in Figure 5. In this case, the 1800 cm^{-1} contribution is not detectable. Therefore, only the 1874 cm^{-1} intensity (integrated over the range ± 5 cm^{-1} around 1874 cm^{-1}) is displayed as a function of time. The best fit of the data is obtained using two slopes indicating two desorption thresholds centered roughly at 220 K and at 250 K.

The situation is similar on flat Al(111) surfaces. A surface dosed at 150L is characterized by the disappearance of both the 1795 and 1870 cm^{-1} modes around 220 K. A saturated surface displays two desorption edges at 220 K and 280 K (instead of 250 K on the stepped surface). This difference between flat and stepped surfaces is consistent with the observation in Figure 3c where the desorption temperature of hydrogen and alanes (dosed at saturation at 250 K) is higher on the flat surface than on the stepped surface. However, the loss of all IR absorption signal at 280 K is still at a lower temperature than the complete H desorption observed at 340 K by TPD.

In summary, the results presented above indicate that atomic hydrogen exposure of an Al surfaces leads to a very complicated situation, with a variety of species. To properly interpret the complex IR spectra, it is necessary to carry out theoretical modeling providing information of the adsorption sites of hydrogen and alanes, the corresponding normal modes, and adsorption energies. In the next section, we discuss a selective list of possible adsorption configurations for hydrogen on the Al(111) surface.

Theoretical Results. 1. Hydrogen on Al. The theoretical investigation of alanes starts with the calculation of vibrational frequencies from H atoms on terraces and atomic steps of Al(111). We find that the all-electron DFT calculated ground-state for a sparsely covered Al surface (one H per unit cell for the current case) is a quasibridging site between two Al atoms tilted toward the three-center hollow site. This multicenter configuration leads to a relatively low vibrational frequency perpendicular to the surface (∼1150 cm^{-1}). This position is slightly different from the three-center site typical of most (111) metal surfaces. In Al, the three-center or hollow site is slightly higher in energy (0.042 eV) compared to the distorted bridging site discovered in our calculations. Adding a polarization p-function on the hydrogen (DNP basis set under GGA-RPBE calculated all-electron ground state) does not change this finding, i.e., the hollow site is not the most stable configuration. The vibrational frequency (1125 cm^{-1}) is significantly lower than that of on-top H-monolayers on an Al surface but is consistent with the previous experimental observation by Paul et al.[9]

Hydrogen has solubility in the bulk metallic lattice and could act as an interstitial impurity. The hydrogen in the Ni(111) subsurface lattice has been studied and detected using EELS and TPD.[30] However, such clear experimental evidence has not been observed in the case of H on Aluminum.[31,32] Crane at al. have shown that the interaction of a low energy Xe beam with an H-saturated Al(111) surface reduces strongly the AlH_3^+ TPD signal, with only a slight decrease of the H_2^+ signal. They conclude that H_2^+ desorption is mostly independent of the amount of aluminum hydrides on the surface and propose that the initial state of H adsorbed on the Al(111) surface could involve subsurface species. In this scheme, the thermal energy of the incoming atomic hydrogen would be sufficient to overcome an adsorption barrier for subsurface sites. These conclusions assume that the AlH_3^+ component of a TPD experiment is representative of all the aluminum hydrides present on the surface. This might not be the case, as indicated by our IR study, since different adsorbed species coexist on the Al surface, leading to a more complicated fit of their TPD data.

From the theoretical point of view, the binding energy, bulk solubility, phonon spectra, and diffusion barrier of hydrogen in Al have been studied in detail by Wolverton et al.[33] It is however worth noting that H has a very low solubility in Al and a 0.4−0.6 eV barrier for interstitial diffusion.

At higher coverage, adsorbed hydrogen prefers a site that is very close to the top site. This site is characterized by an Al−Al−H angle of 95° with respect to surface Al atoms instead of 90° for the ideal on-top site. The calculated vibrational spectrum from an H monolayer with H bound to the top sites is characterized by a combination of modes. The highest intensity mode is the collective out-of-plane vibration of Al−H bonds, calculated to be at 1790 cm^{-1} on flat surfaces. The next important configurations are sparsely populated atomic steps and H-saturated steps on Al(111). The same phenomenon is observed, i.e., when H atoms are bound on sparsely populated steps, the intensity of the out-of-plane vibrations arises from the bridge-bonded H atoms and the vibrational frequency is 1081 cm^{-1}. For a H-saturated stepped surface, the vibrational frequency from the H atoms on the steps is 1849 cm^{-1}. The correlation of the vibrational frequency to the binding energy calculated for these sites is consistent: the stronger binding environment shows a higher vibrational frequency for the Al−H bond. Also, there is a net minimization of energy if the mobile hydrogen atoms migrate on the surface and bind to the steps. We find that the H binding energy on the atomic steps is 3.89 eV compared to 3.03 eV on the flat surface. As a result, it is conceivable that the steps will become saturated before the flat terraces are saturated on an Al surface. The Al adatom-H bonds

(30) Johnson, A. D.; Maynard, K. J.; Daley, S. P.; Yang, Q. Y.; Ceyer, S. T. *Phys. Rev. Lett.* **1991**, *67* (7), 927–930.
(31) Boh, J.; Eilmsteiner, G.; Rendulic, K. D.; Winkler, A. *Surf. Sci.* **1998**, *395* (1), 98–110.
(32) Winkler, A. *Appl. Phys. A: Mater.* **1998**, *67* (6), 637–644.
(33) Wolverton, C.; Ozolins, V.; Asta, M. *Phys. Rev. B* **2004**, *69* (14), 144109.

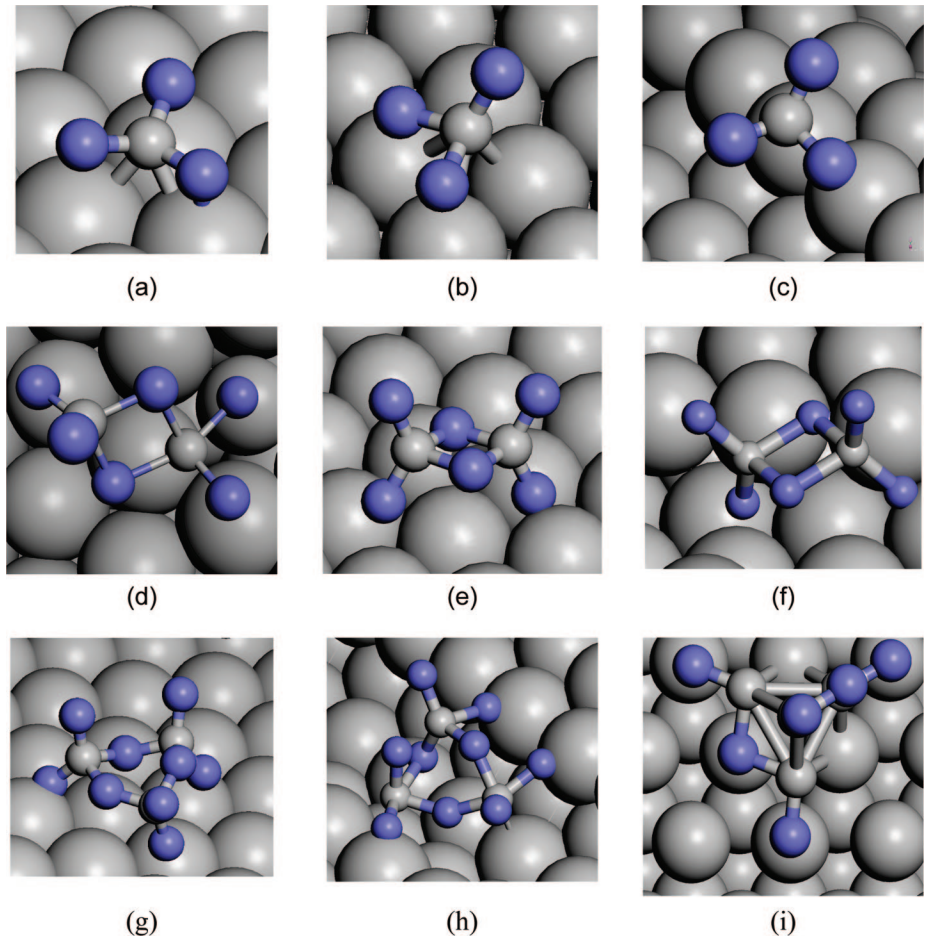

Figure 6. Selected bonding environments for alane clusters on an Al(111) surface including: (a) AlH_3 on semihorizontal ground state, (b) AlH_3 in semivertical tetrahedral binding, (c) AlH_3 on the step, (d) semivertical bridge-bonded Al_2H_6 cluster on terrace, (e) chemisorbed and horizontal Al_2H_6 on terrace, (f) chemisorbed Al_2H_6 attached to atomic steps, (g) chemisorbed Al_3H_9 on the terrace, (h) Al_3H_9 bound to a step, and (i) the Al_4H_6 cluster bound to a surface viewed from the top. It is a *closo*-borane analogue[28,29] recently reported to be stable in gas-phase.

are also stable and have a binding energy between that of a quasibridging and an H-atom bound to the steps. The adatom-H vibrations are similar to those on H-saturated steps, and the calculated frequency for the out-of-plane stretching mode is 1846 cm^{-1}.

2. Physisorbed Clusters. Weakly bound clusters have properties comparable to gas-phase clusters because the interaction with the substrate is negligible. The alanes thus formed will have geometry similar to gas-phase clusters calculated inside the periodic box and will be mobile under thermal excitations. As a result of these added degrees of freedom compared to the chemisorbed clusters, the IR-active normal modes of such mobile alanes should be observable in the experiment if a sufficient number of them are present in the physisorbed state. Table 1 shows the normal modes calculated for some of the stable gas-phase clusters. The aim is to categorize the spectral regions that are detectable by IR when alane clusters are physisorbed. The physisorbed state corresponds to a shallow minimum located 2.8−3.4 Å from the surface (surface Al to cluster H atom distance) that cannot be accurately described by DFT techniques. However, we calculated a 0.12 eV barrier to chemisorption on the Al surface for an unbound AlH_3 cluster even though the overall reaction is exothermic by 0.96 eV. The transition state is located ca. 3.05 Å from the nearest surface atoms where the planar gas-phase AlH_3 cluster begins to distort before chemisorbing in a vertical AlH_3 orientation as shown in Figure 6b. Such a barrier originates mostly from the repulsion between the electrons in the metallic surface and bonding electrons in the alane clusters. These can be balanced by attractive van der Waals interactions at larger separation leading to a physisorbed state. The gas-phase geometry of the AlH_3 clusters must further distort to reach the chemisorption minimum. We believe that the situation for larger alanes is similar and can therefore rationalize the existence of loosely bound alanes on the surface.

3. Role of the Binding Environment. As shown in Tables 1–3, the vibrational frequencies change significantly for a particular cluster when it is bound to an Al (111) surface either on a terrace or at an atomic step. The general trend shows a lowering of the highest-frequency modes for all the clusters studied. This is an indication that the electron density is redistributed between the alane cluster and the Al surface resulting in a changed oscillator strength of the cluster Al−H bonds. The bound clusters differ in their IR signatures significantly compared to their gas-phase analogues owing to the changes in symmetry and differences in their electronic environments on the Al surface. The orientation of the clusters on the surface is also important. For example, the AlH_3 cluster can bind to a terrace either via a bridging bond in a pseudotetrahedral arrangement (identified as $\nu_T(t_d)$ in Table 2) or as an inverted tetrahedron with the Al bound to the hollow site (identified as ν_T(h) in Table 2 and shown in Figure 6b). The previously

Table 2. Comparison of Calculated Vibrational Frequencies of AlH_3 in the Gas Phase (ν_G), Adsorbed on an Al(111) Surface Terrace (two configurations, $\nu_T(t_d)$ and $\nu_T(h)$), and Adsorbed on an Atomic Step (ν_S) Reflecting Changes in the Vibrational Spectra in the New Binding Environment[a]

AlH_3 freq (cm^{-1})				Al_2H_6 freq (cm^{-1})				
ν_G	$\nu_T(t_d)$	$\nu_T(h)$	ν_S	ν_G	ν_T		ν_S	
695.8	613.3	665.8	606.3	616.2	681.4	1450.5	637.8	1163.3
780.8	935.1	672.0	673.1	700.0	705.5	1535.9	651.9	1349.4
782.5	1027.3	1721.7	1088.8	834.8	762.1	1800.2	686.2	1553.2
1889.9	1367.4	1807.3	1427.2	1245.3	1022.0	1860.8	732.6	1597.9
1902.9	1406.3	1816.1	1819.0	1331.5	1097.8	1878.9	934.1	1779.2
1914.0	1824.9		1839.0	1416.7	1260.6		940.2	1832.4
				1932.4	1318.2		1289.9	1869.8
				1958.6				

[a] Only frequencies above 600 cm^{-1}, reflecting the relevant high-frequency modes, are tabulated.

Table 3. Calculated Vibrational Frequencies in the 1500−1950 cm^{-1} Range for the Spectrum of Larger Alanes Species[a]

$\nu_P(Al_3H_9)$	$\nu_T(Al_3H_9)$	$\nu_S(Al_3H_9)$	$\nu_S(Al_4H_6)$
1046.9	1000.8	1071.4	1009.3
1681.9	1092.4	1428.4	1205.9
1750.9	1114.9	1443.2	1310.3
1763.9	1364.0	1451.2	1398.2
1887.5	1369.1	1530.9	1469.2
1894.4	1542.4	1556.5	1511.0
1904.8	1560.5	1577.3	1774.0
1911.9	1634.9	1733.3	
1917.6	1716.4	1844.0	
1923.4	1821.0	1929.5	
	1840.4		
	1881.9		

[a] The vibrational modes of Al_4H_6 cluster is also calculated because it has recently been reported[28,29] in gas-phase experiments. The subscript P is for physisorbed, T for terrace, and S for modes from clusters bound to steps.

observed experimental IR active modes for gas-phase Al_2H_6 at 1932, 1915, 1408, and 1268 cm^{-1} (obsd column in Table 1) can be mapped onto similar modes at 1879, 1861, 1451, and 1290 cm^{-1} (Table 2) of an Al_2H_6 cluster bound to the terrace. For Al_3H_9 the trend is slightly different due to the added complexity of the structure compared to Al_2H_6. This is evident in the nonlinear nature of the shifts in the calculated vibrational frequencies shown in Tables 1 and 3 for gas-phase and surface-clusters, respectively. The situation for a cluster bound to an atomic step is more complicated. New modes are generated, and although they are not as strong as the gas-phase modes, they broaden the spectrum significantly.

Which Modes Are Surface IR Active? We first discuss the IR vibrations that are likely to be observed from alane clusters absorbed on the surface. Tables 2 and 3 list the calculated frequencies for different normal mode vibrations of chemisorbed alane clusters. The Al surface, like any other metal surface imposes a selection rule for IR spectroscopy. Only the vibrations with dipole moments perpendicular to the surface can be excited. In order to provide the best assessment of complex surface phenomena, we first discuss each calculated cluster and its most probable IR-active modes. If the most intense modes are not present in the experimental spectra, it is likely that the cluster is not present at all. We have divided the discussion of probable modes for clusters bound to terraces and steps sequentially. Then we discuss the experimental identification of different regions of the spectra at different temperatures. Finally we analyze the energetics of alane binding, growth, and desorption on the Al surface as calculated using all-electron DFT-models for surfaces and individual clusters. The chemistry of alanes on the Al surface is the net result of two competing exothermic processes: (a) adsorption on the Al surface, and (b) oligomerization with other alanes, e.g., two AlH_3 clusters forming Al_2H_6. The surface IR data provide a link to identify these processes and give an indication of the surface chemical dynamics of alanes. At the same time, the gas-phase modes are excited when the cluster is physisorbed and is relatively free to rotate and translate. We will describe the surface IR active modes of chemisorbed clusters next as all the IR active modes and their intensities for the physisorbed or gas-phase clusters have been provided in Table 1.

1. Clusters on Terraces. Case 1: AlH_3. The most stable binding geometry for AlH_3 is the horizontal cluster with a slightly distorted C_3 symmetry. In terms of binding, the cluster has a nearly octahedral coordination environment when the octahedron is seen along the C_3 axis. The Al atom in the AlH_3 unit is bound to three surface Al atoms and the three H-atoms from the cluster completing the coordination. As a result of the orientation of the H-atoms with respect to the Al(111) surface, the normal mode displacement vectors are not completely vertical, however, they have components perpendicular to the Al surface especially for the symmetric stretch mode which appears at 1807 cm^{-1} (see Table 2). The mode at 1824 cm^{-1} is the asymmetric stretch involving two Al−H bonds and does not have any net perpendicular dipole moment. The second binding possibility is the vertical cluster with a dangling Al−H bond perpendicular to the surface and the other two Al−H bonds forming bridging bonds with the Al surface. The intensity of the symmetric stretching mode involving this dangling Al−H bond, calculated to be at 1824 cm^{-1}, is strong. The symmetric stretch of the bridges (1406 cm^{-1}) might also have components perpendicular to the surface but are less intense.

Case 2: Al_2H_6. The horizontally bound Al_2H_6 oligomer is again the most stable binding configuration; however the situation is complex due to the distortion from the isolated cluster geometry. We find that the force constants for the two dangling Al−H bonds are different and have two different symmetric stretch frequencies at 1823 and 1879 cm^{-1}. Both of these modes have vertical dynamic dipole components and should be visible in surface IR experiments.

Case 3: Al_3H_9. Evidence for the presence or the absence of Al_3H_9 is dependent primarily on its terminal H atoms as well. For example, for physisorbed clusters, the existence of the 1911, 1923, and 1917 cm^{-1} modes is important. The 1881, 1840, and 1820 cm^{-1} modes from the chemisorbed cluster also have higher intensity due to their vertical displacement vectors of the three terminal Al−H bonds. The spread in the vibrational frequencies of the terminal Al−H bonds shows the effect of binding and distortion. The strongly bound ends of the cluster have a weaker terminal Al−H bond and thus a lower vibrational frequency. As a result, surface IR frequencies seem to have an inverse correlation to the strength of the bond between the alane cluster and Al surface.

Case 4: Others. The other environments considered include the Al adatom-H or the Al−H vibrations from terraces, and the surface-adsorbed H atoms. The Al−H vibrations are around 1846 cm^{-1}, and they should be IR active. The same is true for surface H atoms, although their frequency shifts with surface coverage. For monolayer coverage, the modes are between 1750−1800 cm^{-1}, and not all modes are surface active. Interestingly, a single H atom per unit cell on the 3-fold site has a vibrational frequency of 1150 cm^{-1}. It is therefore very

difficult to pinpoint surface hydrogen environments without first determining surface coverages. The work by Paul et al. shows the several factors that can change Al−H vibrations on an Al surface.[9] The other probable species are the substoichiometric alanes. Among many possibilities, AlH_2^+ for example as a gas-phase species is linear; bending and the asymmetric stretch modes are calculated at 550 and 2122 cm^{-1}. When chemisorbed, the horizontally chemisorbed AlH_2^+ cluster forms Al−H−Al bridging bonds between the cluster and surface. The calculated along-the-surface vibrational modes (symmetric and asymmetric stretch) are at 1335 and 1322 cm^{-1}, respectively. They are unlikely to have any dipole signature perpendicular to the surface. The out-of-plane vibrations are at much lower frequencies at 892 and 915 cm^{-1} and will be hard for us to detect as described in the Experimental Section. The vertical chemisorption results in a cluster with a free dangling Al−H bond with stretching mode frequency at 1886 cm^{-1}.

2. Clusters at Steps. Case 1: AlH_3. Only the symmetric stretch mode involving the unbound (free) Al−H at 1839 cm^{-1} is IR active when an AlH_3 cluster is bound to an atomic step. The cluster Al atom bound to a step (Figure 6c) has a pseudotetrahedral symmetry. It forms an Al−H−Al bridge bond with an Al atom in the step. The cluster Al also has a bonding interaction with a step Al atom.

Case 2: Al_2H_6. For Al_2H_6 there are two modes that are IR active at 1869 and 1832 cm^{-1} when it is bound to a step. They correspond to the stretching modes of the two vertically oriented free terminal Al−H bonds. The attachment (Figure 6f) of the Al_2H_6 takes place via two Al−H−Al_S bridge bonds and one of the cluster bridge bonds also binds as a bridge between the two Al atoms from the steps.

Case 3: Al_3H_9. The Al_3H_9 cluster adsorbed at steps constitutes too large a molecular cluster for our current unit cell size. As a result, there is an interaction with the periodic image of the step edge in the adjacent cell, leading to an artificially narrow distance between the steps as shown in Figure 6h. In general, the binding with the step edge and the interaction with terrace were converged in our calculations. With that caveat, the symmetric stretch modes involving the free Al−H vibrations are at 1923 and 1844 cm^{-1}. The 1923 cm^{-1} mode has a large dipole moment perpendicular to the surface (Figure 6h) compared to the 1844 cm^{-1} mode. The 1733 cm^{-1} mode involves a combination mode of the bridging group and the free Al−H bonds, which may also have a cooperative dipole moment in the vertical direction.

Case 4: H on the Steps. The H atoms bound to the steps are oriented at an angle with respect to the surface normal. However, the hydrogen atoms from a saturated step have symmetric stretching vibrations that are IR active in the vicinity of 1854 cm^{-1}.

3. Adsorption Energy of Chemisorbed Clusters. Table 4 compares the calculated binding energies of a series of alane clusters bound to an Al(111) surface. These binding energies are relevant to understanding the usefulness of such a system for hydrogen storage since they control in principle the release of hydrogen. As seen in Table 4, there is a wide range of binding energies arising from the various cluster geometries dictated by the optimized binding geometries on an Al(111) terrace or atomic step considered in this work. We find that semihorizontal AlH_3 clusters are very strongly adsorbed (−3.87 eV) compared to the vertical AlH_3 clusters (−0.91 eV) on the terraces (Figure 6). The bound vertical AlH_3 cluster has a lower barrier to formation from a gas-phase planar AlH_3 molecular cluster. For the ground-state semihorizontal cluster, there is a very high barrier to formation. Such a ground state will most likely be absent under the low-pressure conditions studied experimentally in this work. Its binding on the steps is stronger (−0.99 eV) compared to vertically chemisorbed AlH_3, which suggests that AlH_3 clusters will tend to form at the steps first. The Al_2H_6 cluster, on the contrary, is more stable (−2.16 eV) on the terraces relative to the steps (−1.71 eV), but the difference can be due to the repulsion and geometric constraints for chemisorbing in a configuration shown in Figure 6f. Also, the binding energies of the Al_2H_6 cluster at different sites suggest that it will first form as an angularly bound cluster with two Al−H−Al bridge bonds with the surface. The formation of a horizontal Al_2H_6 cluster on the surface is expected to have a significant activation barrier. This is due to the initial increase in the repulsive interaction while transforming Al_2H_6 bound to the surface in a semivertical (−0.22 eV) geometry to the energetically favored distorted horizontal geometry with respect to the Al(111) surface. The Al_3H_9 cluster also finds stable minima on both steps (−2.46 eV) and the terraces (−2.23 eV) on an Al (111) surface, but in this case binding to a step is slightly favored. These results show that larger 3D clusters such as Al_4H_6 (see Figure 6), recently reported in the gas phase by Li et al.,[29] can also be stable on the surface in a chemisorbed state. However, it will be difficult to identify its IR signature from the three-center and bridging hydrogen atoms (Figure 6i).

Table 4. Binding Energies of Various Alane Clusters to Different Al(111) Environments Calculated from Computed Energies as Follows: E_{bind} = [E(cluster on surface) − E(cluster) − E_{Al}(surface slab)].

	environment	binding energy[a] (eV)
1.	AlH_3 on terrace (inverted t_d)	−3.87
2.	AlH_3 on terrace (vertical t_d)	−0.91
3.	AlH_3 on step	−0.99
4.	vertical Al_2H_6 (terrace)	−0.22
5.	Al_2H_6 on terrace	−2.16
6.	Al_2H_6 on step	−1.71
7.	Al_3H_9 on terrace	−2.24
8.	Al_3H_9 on step	−2.46
9.	Al_4H_6 on terrace	−1.32
10.	Ad-atom or Al−H	−3.54
11.	H-on-steps	−3.90
12	H-on terrace	−3.05

[a] The values are not zero-point energy (ZPE) corrected. The correction from ZPE is small (<0.2 eV), and they do not change the ordering in any significant way.

Discussion

General Trends. The picture derived from our experimental FTIR results points to a complex system where several adsorbed species coexist on the surface. Their relative concentration clearly depends on the step density, the surface coverage, and the temperature. The theoretical models considered in this study also show that there are many possible stable environments for hydrogen adsorption on an Al(111) surface, from single H to larger alanes. A general trend for the calculated frequencies can be drawn from these models.

First, modes associated with bridge-bonded H occur around 1100 cm^{-1} (1150 cm^{-1} on terraces and 1080 cm^{-1} on step edges) at low coverage. Since the H coordination is high and hydrogen relatively close to the surface (higher screening), these modes have a weak (screened) dipole moment and are generally not observed in IR. They can be, however, detected with EELS that is more sensitive to such low-frequency modes.[9] Closer to

saturation, collective oscillation modes are found at higher wavenumbers at step edges (1854 cm^{-1}) or terraces (1849 cm^{-1}).

In the case of alanes, there are two distinct environments for hydrogen: terminal hydrogen atoms and bridging hydrogen atoms. For small *chemisorbed* alanes (AlH_3 and Al_2H_6) terminal hydrogen atoms have bands in the 1850 cm^{-1} region for both step and terrace sites. Bridging hydrogen atoms are characterized by lower frequency vibrations (typically below 1800 cm^{-1}). The only exception is the artificially high frequency of a specific mode of terminal hydrogen in Al_3H_9 because the 11.45 Å × 11.45 Å surface unit cell used in the calculation is too small. As a result, there is some interaction between the optimized geometry of Al_3H_9 and the step edge in the periodic image. The calculated frequencies for all the other modes are not substantially affected by this problem. Using a larger surface super cell size makes calculations computationally very expensive by the addition of 48 more Al atoms to the unit cell and is not justified at this point.

When alanes are not chemisorbed, but remain only weakly adsorbed, they can be modeled by simple molecular alanes, characterized by higher frequencies of the terminal hydrogen vibrations (>1915 cm^{-1}), much higher than what is calculated for the chemisorbed species. All the calculated frequencies obtained using a DFT approach are typically higher than observed experimental values due to the tendency of GGA-DFT to overbind the molecules. A correction factor is therefore necessary to compare with experiment, best determined by examining the difference between calculated and measured frequencies of molecular alanes. Given the high reactivity of alanes, only IR spectra of alanes trapped in rare gas matrices are available.[31] The typical deviation from gas phase frequencies of rare gas matrix data is typically of order 1 to 2%,[34] Therefore, we have to apply a correction of at least −20 cm^{-1} to our calculated gas phase values. Since the error in the estimation of frequencies in an electronic structure calculation depends on the overall electronic description of the bonding, a specific correction applies to only one type of bonding configuration, so that different correction factors are required for vibrations of terminal or bridge hydrogen atoms, respectively.

Assignments of IR Spectra. The main difference between the IR spectra of the H-exposed flat and stepped Al(111) surfaces is the presence of a strong 1795 cm^{-1} peak for a highly stepped surface after a 15L exposure (Figure 1). At such a low coverage, this mode must be associated with the step adsorption of either atomic H (1854 cm^{-1}) or a small alane such as AlH_3 (1839 cm^{-1}). The binding energy of a hydrogen atom at a step edge being 0.86 eV higher than on a terrace on-top site, step edges will be most likely saturated first. At higher coverage, the increasing density of H on the step edges could favor AlH_3 formation. Using this observation, we establish the correction to our calculated wavenumbers for a single H on Al at saturation or the terminal Al−H vibrations of an alane to be in the range of −40 cm^{-1} to −60 cm^{-1}, i.e., −50 cm^{-1} on average. Therefore, all the calculated values for terminal hydrogen modes presented in Tables 1–4 should be lowered by 50 cm^{-1} to compare to experimental spectra. This important correction clearly shows that there is no observable detection of chemisorbed alanes. Instead, the range of observed terminal H frequencies can only be accounted for by terminal hydrogen atoms of gas-phase or weakly adsorbed molecules.

For instance, the terminal hydrogen mode for gas-phase AlH_3 (calculated at 1914 cm^{-1}) and gas-phase Al_2H_6 and Al_3H_9, modes (calculated at 1959 cm^{-1} and 1923 cm^{-1}, respectively) should be shifted to 1864 cm^{-1} for AlH_3 and to 1909 cm^{-1} and 1873 cm^{-1} for Al_2H_6 and Al_3H_9, respectively. The mode observed at 1860 cm^{-1} could therefore be associated with the terminal hydrogen of weakly adsorbed AlH_3 and Al_3H_9. There is also a possibility that the vertically chemisorbed AlH_2^+ species can be present on the surface as well due to the proximity of the calculated out-of-plane stretching vibration at 1886 cm^{-1} to the experimental peak. However, since this mode appears at relatively low coverage (after ∼15L exposure), it is more likely due to a physisorbed or a weakly interacting AlH_3 species. The transition from AlH_3 chemisorbed on a step edge to AlH_3 physisorbed can be facilitated by the repulsive interaction of chemisorbed AlH_3 molecules when the step edge is saturated. Although the full reaction path is not understood, the data support this extraction mechanism of AlH_3 from a step edge, which may be the cause for the apparent etching of the Al(111) surface step edges during H exposure (seen with STM).[12] At higher coverage, the shoulder at around 1900 cm^{-1} can be attributed to the vibration of the terminal hydrogen of Al_2H_6. The situation is less clear in the bridge H part of the spectrum because only a very broad feature is observed (centered around 1600 cm^{-1}). It is possible that the bridging hydrogen from the Al−H−Al linkages in the larger alanes oriented in various metastable binding configurations contributes to this broad feature.

On flat surfaces, the step density is low. It is therefore not possible to detect H or alanes chemisorbed on step edges (∼1795 cm^{-1}). On the other hand, there is a measurable absorption in the spectral region corresponding to bridging hydrogen at much lower exposures (e.g., 30L) than what is seen on stepped surfaces. This indicates that larger alanes can be formed faster or at least at lower coverages. Since larger alanes are believed to be formed by oligomerization of smaller alanes, this observation suggests that AlH_3 and small alanes are more mobile on flat terraces than on highly stepped surfaces. It was previously calculated that the diffusion of chemisorbed alanes through the Al−H−Al bridging sites provides a low energy diffusion route for the entire cluster on the Al surface.[1,2] The mobility of weakly bound clusters should be even higher than for these chemisorbed species. So, the above observations suggest that steps provide a barrier for the diffusion of both chemisorbed and weakly bound alanes. As a result, steps get saturated first and it is possible that alanes are formed from the steps. This observation is important for nanoscale Al which is proposed for a lower H_2 pressure synthesis of bulk AlH_3 phases. In nanoscale Al, the H-saturated edges can lead to more efficient formation of alanes compared to bulk Al.

Thermal Study and Desorption Process. In order to enhance the mobility of small alanes and to test their role in the formation of larger alanes, we have performed temperature dependence studies by exposing both flat and stepped Al(111) surfaces to atomic hydrogen at 180 K, 220 K, and 250 K. On stepped surfaces (Figure 4), at 220 K, larger alanes, characterized by their broad bridge hydrogen contribution around 1600 cm^{-1} are already present after 15L exposure whereas they were absent at 90 K. Their spectra are really similar to those obtained on a flat Al surface at 90 K, indicating a possible enhancement of the mobility that compensates for the smaller size terraces of the stepped surface. At 250 K, the high-wavenumber bands become broader and there is a loss of IR absorption intensity

(34) Jacox, M. E. *Chem. Soc. Rev.* **2002**, *31* (2), 108–115.

around 1600 cm^{-1}, suggesting that large alanes are modified (possible dissociation into smaller alanes that can partially desorb). On the flat surface, the spectra obtained at 180 K, 220 K, and 250 K (not shown here) are very similar to what is observed at 90 K, showing that at 90 K on the flat surface, the species have probably already reached a dynamical equilibrium.

Now that we have tentatively assigned the IR spectra to various species, we can try to characterize the modifications of these species on the surface by looking at the evolution of the full IR spectra as a function of temperature (Figures 4 and 5). On the stepped surface dosed 150L at 90 K, the IR spectrum is composed of a band at 1795 cm^{-1} corresponding to the H/AlH_3 chemisorbed on step edges and of a band at 1870 cm^{-1} corresponding to the weakly bound AlH_3. As soon as the temperature increases, the chemisorbed H/AlH_3 feature decreases while the physisorbed AlH_3 fingerprint starts growing to reach a maximum at 160 K. This supports the idea of a transition mechanism from chemisorbed species on the step edges to weakly bound AlH_3 that is mobile on terraces. Above 160 K, the IR intensity diminishes and completely disappears at 220 K. This result is in apparent disagreement with previous TPD data showing a desorption peak at 340 K for H_2 and alanes fragments from Al(111). This observation suggests that it might be possible to have hydrogen-containing species (alanes) with undetectable IR modes. For example, the 2-fold bridge-bonded H atoms or some form of alanes with vibrational modes parallel to the surface are not detectable due to the surface selection rule. Thus, surface species including the alanes could get transformed above 220 K into other alanes without any significant IR transition perpendicular to the surface, such as *closo*-alanes. These species have stoichiometries such as Al_nH_n or Al_nH_{n+2}, etc. (for $n > 1$), and are devoid of terminal hydrogen atoms.[35] We have studied only one such species, Al_4H_6 as shown in Figure 6i which has been identified experimentally even in the gas phase.[28,29] This species tends to adsorb in a structure parallel to the surface, exhibiting no IR active mode, making it impossible to follow the evolution of alanes beyond this point.

As a result, it is possible that the loss of IR intensity observed upon annealing to 220 K is due to the reduction of large alanes (by formation of molecular H_2) into closoalanes. The binding energies of chemisorbed alanes (see Table 4) are much too high to allow desorption at 220 K. What emerges from our study is that the 0 K structures are not stable at higher temperatures. Surface hydrogen atoms (which are very strongly bound to the surface by 3.1 to 3.8 eV) can diffuse and recombine easily to form H_2 that can then desorb because it is only weakly bound to the surface. Larger alanes may be able to shed-off their terminal hydrogen atoms as H_2 to form *closo*-alanes, while smaller alanes may be able to desorb under certain circumstances (if they remain weakly bound or depending on the site or overall H coverage). The temperatures at which alanes have been observed to desorb in the literature[9,10] is more consistent with low binding energies, such as <0.1 eV associated with weakly bound (mobile) alanes than with chemisorbed alanes, in agreement with our IR observations.

On a saturated stepped surface (Figure 6), the 1795 cm^{-1} peak corresponding to chemisorbed species on the steps is not visible anymore and only the 1870 cm^{-1} peak is monitored as a function of temperature. Similarly to what was observed previously, this peak goes through a maximum at 160 K and then decreases at 220 K. After 220 K, another desorption edge is visible at 250 K, probably due to the decomposition of larger alanes. The fact that some IR absorption intensity remains detectable up to 250 K supports the idea that alanes do remain adsorbed at such high temperatures. While at low coverage, they can form *closo*-alanes that are not detectable with IR spectroscopy; at higher coverage some of them are detectable depending on stoichiometry and arrangement of the clusters. For all these transformations as temperature is increased, it is likely that entropic factors dominate the process, opening channels for structural evolution, aggregation and dissociation, and ultimately desorption.

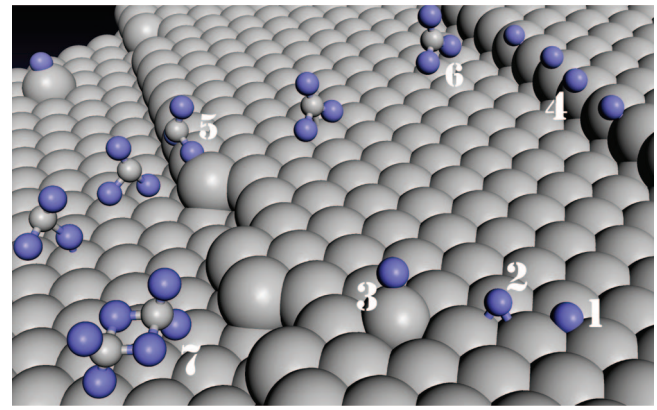

Figure 7. Atomic H species and formation of alanes on the Al(111) surface: (1) 3-fold bridge H, (2) quasibridge H, (3) H on Al adatom, (4) H on step, (5) AlH_3 chemisorbed on a step, (6) AlH_3 physisorbed on a terrace, (7) Al_2H_6 physisorbed on a terrace.

Summary and Conclusion

The overall picture of alane formation and growth is a net result of competitive dynamics involving chemisorbed hydrogen atoms, alane clusters, and subsequent reconstruction of a highly unstable Al surface. Starting from very low temperatures and low H coverages, the Al surface undergoes changes progressively and produces a complex set of vibrational environments explored using a combined surface IR and first-principles techniques, as summarized in Figure 7. At 90 K, the single crystal surface exposed to hydrogen shows a preferential adsorption on step edges [Figure 7(4)] and Al ad-atoms [Figure 7(3)] as energetically favorable binding sites for hydrogen. It is likely that even at these low temperatures H atoms migrate relatively freely aided by low diffusion barriers for H in Al and possible tunneling of H. Experimentally, hydrogen atoms are observed on quasibridge position [Figure 7(2)] on terraces by EELS (and not in 3-fold position [Figure 7(1)]) and at steps [Figure 7(4)] by IR absorption measurements (our study). The instability of the step edges due to H saturation and lower diffusion barriers is a probable reason that leads to the creation of smaller alanes such as AlH_3 [Figure 7(5)]. With increasing coverage, we can identify smaller alanes as physisorbed clusters on flat terraces [Figure 7(6)] and some chemisorbed on the step edges [Figure 7(5)]. The transformation of chemisorbed hydrogen into chemisorbed AlH_3 (at steps) and then into weakly bound AlH_3 that can migrate to surfaces is not fully understood but is most likely related to the facile insertion of H below the top Al layer and repulsive interaction of various H species at higher local step coverage. Our calculated results indicate that vibrational modes in the physisorbed clusters are similar to the gas-phase clusters since there is no net transfer of electron

(35) Charkin, O. P.; Klimenko, N. M.; Moran, D.; Mebel, A. M.; Charkin, D. O.; Schleyer, P. V. R. *J. Phys. Chem. A* **2002**, *106* (47), 11594–11602.

density to the surface to affect the oscillator strength for relatively intense terminal Al−H stretching modes. Even an all-electron DFT calculation such as the one used in this work is not adequate to address the nature of this physisorbed minimum and to estimate all the possible degrees of freedom for such a cluster. Our calculated results can provide an estimate for the barrier (0.11 eV) to overcome to reach a chemisorbed state for AlH_3. The presence of this barrier may explain why higher hydrogen pressures are necessary for the formation of the bulk aluminum hydride phase. The surface at higher hydrogen coverage shows a broad distribution of IR intensities in the range of 1600−1700 cm^{-1} attributed to different combinations of the vertical vibrational modes of the Al−H−Al bridge bonds present in larger alane clusters, which develop upon higher exposures [Figure 7(7)].

The *thermal desorption* is also highly complex and involves multiple processes occurring simultaneously. Because of the broad nature and higher noise in the near room temperature IR absorption spectra, we cannot develop an exact step-by-step mechanism of desorption. A plausible mechanism derived from examining the DFT-calculated binding energies is that most of the alane clusters dissociate and eventually desorb from the surface with a desorption maximum around 220 K. Starting from a saturation exposure at 90 K, i.e., with more than one hydrogen monolayer (i.e., more H than surface Al sites), there is formation of alane, adatom-H, and Al−H−Al bridging networks on a highly disordered Al surface. As the temperature increases during the desorption studies, it is likely that the alane clusters, subsurface and surface H atoms, all prefer to recombine into molecular H_2 as an entropically favored route. This process has been studied by Crane et al.[36] and Boh et al.[31] where the authors found an unusual zero-order reaction kinetics for H on Al(111). The physisorbed clusters are also likely to be desorbed as stable gas-phase clusters such as AlH_3 and Al_2H_6 previously identified as present in the desorbed medium.[10] During this desorption and disintegration of alanes into smaller alanes, the Al surface loses coverage of H-atoms and terminal H atoms from alane clusters around 250 K, accounting for the complete loss of IR absorption. The thermal desorption and evolution of hydrogen and alanes results in very low density of hydrogen at steps, as evidenced by relatively low IR absorption upon extended H dosing of stepped surfaces.

The alanes when chemisorbed are highly stable if we just consider the calculated binding or absorption energies at 0 K. The thermal evolution observed in the present IR absorption studies suggest that the entropic driving force (the $T\Delta S$ term in $\Delta G = \Delta H_{abs} - T\Delta S$) strongly influences the desorption process of alanes. To reconcile some of the difference in desorption temperature reported in the literature, we believe that the rate of desorption is an important variable in this process. Since the temperature ramp is extremely slow in our study, the process is near-equilibrium conditions and is characterized by a markedly higher rate of recombination to molecular H_2.[36] This may be a result of the subsurface H atoms that can possibly exist in the interstitial positions of bulk Al lattice and diffuse to the top layer allowing a higher rate of recombination with terminal H atoms from the alane clusters. Of course, the IR studies are not sensitive to the presence of *closo*-alanes, which complicates the development of a comprehensive mechanism.

While we have attempted to provide an overall mechanism for H adsorption and desorption on Al surfaces, there are still several important limitations in our work that make it difficult to derive a more quantitative picture: (i) even after producing the first-principles based map of the vibrational frequencies and carefully calibrated surface IR spectrum, it is nearly impossible to quantify the nature and concentration of the majority of alanes at higher H coverages; (ii) it is still difficult to estimate the degree of dipole−dipole coupling between modes and the resulting shifts in the vibrational modes because an exact calibration of surface coverage is not possible without calibrated TPD; (iii) the desorption study is not done at a steady state or a linear rate of heating. As a result, a more thorough analysis of the rate equations and desorption curves from desorption barriers of different known species could not be performed in the current work.

Hydrogen Storage Research and Implications. The work presented here is an in-depth investigation of the alanes on Al surfaces using surface IR and first-principles techniques to provide an understanding of the stability and growth of alanes as a preamble to uncovering their probable role in mass transport in hydrogen storage reactions in alanates. Alanes as molecular clusters desorb near room temperature as an indication of their thermal instabilities in the Al metal. We also observe that physisorbed clusters play a dominant role and may be formed subsequent to hydrogen chemisorption. The mechanism and role of such physisorbed species is very important for the reversible hydrogen storage reaction in $NaAlH_4$, where the alanes are produced at much higher pressures and temperatures. We can extrapolate from this study the following features that will be valid under the reaction conditions: (a) there is no kinetic barrier for alane formation in Al once the molecular hydrogen becomes atomic hydrogen (H_2 to atomic H transformation was not examined in our current low pressure study), (b) there is a significant number of weakly bound or physisorbed alanes present on the surface that are highly mobile (i.e., preserve both rotational and translation degrees of freedom that facilitate mass transport), (c) higher H_2 pressures may facilitate hydrogen and alane chemisorption although stability of larger clusters above room temperatures is highly unlikely. There is growing evidence from kinetic studies of hydrogen storage reactions in alanates that diffusion of alanes is very important in the rate equations.[37] Many chemisorbed species with higher binding energy but not detected in this current work at low coverages using surface IR might become very important in future high-pressure, in situ studies of hydrogen storage reactions in Al and alanates as a whole.

Future Studies. Alane formation on single-crystal Al(111) constitutes the essential element for H_2 loading for alanates, and therefore the fundamental understanding of this process is required to study of the effects of H_2 chemisorption catalysts such as Ti and Zr used in the alanates. This ongoing effort will further advance our ability to develop better materials for reversible hydrogen storage as hydrides and complex metal hydrides.

Acknowledgment. This work was performed under the Hydrogen Fuel Initiative Award (BO-130) of the U.S. Department of Energy and supported by Division of Chemical Sciences, Office of Basic Energy Sciences. S.C. acknowledges ONR grant N00014-03-1-0247.

JA800136K

(36) Crane, E. L.; Nuzzo, R. G. *J. Phys. Chem. B* **2001**, *105* (15), 3052–3061.

(37) Lohstroh, W.; Fichtner, M. *Phys. Rev. B* **2007**, *75* (18), 184106.

(38) Kurth, F. A.; Eberlein, R. A.; Schnockel, H.; Downs, A. J.; Pulham, C. R. *J. Chem. Soc., Chem. Commun.* **1993**, (16), 1302–1304.

(39) Duke, B. J.; Liang, C. X.; Schaefer, H. F. *J. Am. Chem. Soc.* **1991**, *113* (8), 2884–2890.